

## Effect of Synthesized Iron Oxide Nanoparticles on Mungbean and Okra Seed Germination

ARCHNA BHATIA, SONIKA, RAJNI AND RACHNA BHATERIA\*

Department of Environmental Sciences, Maharshi Dayanand University, Rohtak-124 001 (Haryana), India

\*(e-mail : bioremediationlab.mdu@gmail.com; Mobile : 92546 45473)

(Received : October 15, 2022; Accepted : November 21, 2022)

---

### ABSTRACT

In the present study, iron oxide nanoparticles were synthesized by using chemical reduction method. Effect of iron oxide nanoparticles with different concentrations i.e. 150 to 600 mg/l on mungbean and okra seed germination was evaluated. Around 100% germination rate and highest germination index were observed in okra and mungbean at 450 and 600 mg/l iron nanoparticles concentration, respectively. After germination maximum shoot elongation was observed at 150 and 600 mg/l iron oxide nanoparticles concentration in mungbean and okra, respectively, while maximum root elongation was observed at 450 mg/l in mungbean and 600 mg/l in okra seeds. Maximum fresh and dry biomass was observed at 150 and 450 mg/l in mungbean and okra, while minimum was observed at 600 mg/l iron oxide nanoparticles concentration in germinated seeds i.e. mungbean and okra. Maximum shoot iron content was observed at 300 mg/l in okra and 600 mg/l in mungbean, while maximum root iron content in both mungbean and okra was observed at higher concentrations i.e. 600 mg/l. No obvious phytotoxicity to okra and mungbean at lower concentrations was observed.

**Key words:** Iron oxide nanoparticles, seed germination, growth parameters, translocation

### INTRODUCTION

Nanotechnology is the advance and modern technology which involves the study of scenario and advancements of materials at the nanoscale. During the past several years, nanotechnology has gained significant awareness in various scientific disciplines e.g. medicine, technology and material advancement. Nanoparticles are fundamental unit to modern science and technology. Among the latest innovations, the nanotechnology inhabits a leading position in various interdisciplinary areas of research with important commercial and other applications. The nanoparticle technology draws attention of scientists, researchers and other technologists towards itself due to its new and high tech applications in biotechnology, biology, physics, chemistry, colloidal science, earth science, etc. and in other new innovative fields which form new generation high tech products used in day today life. With increasing applications of iron-based nanoparticles in various fields, its use on environmental implications, particularly ecotoxicological effects on living organisms in different ecosystems have been aroused (Yirsaw *et al.*, 2016; Lei *et al.*, 2018; Sun *et al.*, 2020).

Iron is known as one of the most extensively used abundant elements on earth (Zahra *et al.*, 2021; Tighe-Neira *et al.*, 2022). Iron is important for living organisms as it plays an important role in the metabolic processes like DNA synthesis, photosynthesis and respiration, also has importance in numerous physiological and biochemical pathways in plants. The different biological actions in plant systems, including cellular enzymes in organelles that are crucial to respiration, photosynthesis, the quality of plant products, etc., depend on iron as a vital micronutrient (Briat *et al.*, 2015). For plant development and metabolism, it is the third most important nutrient. In aerobic soil, it is generally found in Fe<sup>3+</sup> state. Iron is a component of numerous prosthetic groups and enzymes, and it also triggers a number of metabolic processes. The iron solubility in soil and the requirement for iron by plants are out of balance, which results in chlorosis. Biological activity of iron is less due to the formation of insoluble ferric compounds at the neutral pH, in well aerated soils. It is essential for extensive range of biological and physiological processes in the plants as it is a constituent of numerous essential enzymes such as cytochrome of

“electron transport chain” in chloroplasts and mitochondria (Tighe-Neira *et al.*, 2022). It is present in formation of chlorophyll in plant and is required for proper function and structure of chloroplast (Rout and Sahoo, 2015). Iron oxide nanoparticles have a greater potential for different applications with fast progress of nanotechnology and iron nanoparticles used extensively in various industries, and biomedical and commercial application. Due to their magnetic property and high reactivity, iron nanoparticles are used as a highly efficient remediation agent for environmental applications.

In plant, iron is elaborated in numerous physiological procedures including chlorophyll, redox reactions and biosynthesis (Zargar *et al.*, 2015). Iron insufficiency not only influences development and growth of plants but also leads to anaemia in human and animal. So, iron plays significant role in development and plants growth. Iron nanoparticle generally involves  $\text{Fe}_3\text{O}_4$  magnetite,  $\alpha\text{-Fe}_2\text{O}_3$  hematite and  $\gamma\text{-Fe}_2\text{O}_3$  maghemite among these forms, magnetite and maghemite are the popular phases of iron nanoparticles. The magnetic properties of iron oxide nanoparticles are affected by particle's shape and size. Iron nanoparticle can simply oxidized in presence of air and result in the damage of magnetism. The unique characteristics of nanoparticles are size, shape, high surface area, high reactivity, tunable pore size, structure, toughness and other surface properties (Siddiqui *et al.*, 2015; Khan *et al.*, 2019; Tighe-Neira *et al.*, 2022). All these properties can cause various impacts which can be negative (including functional and structural damage) positive or neutral in the environment and therefore in food crops also (Da Costa and Sharma, 2016; Sarmast and Salehi, 2016; Tripathi *et al.*, 2017; Tighe-Neira *et al.*, 2018).

Mungbean or green gram [*Vigna radiata* (L.) R. Wilczek] has been grown in India and thought to be a native crop of this country. In particular, for its high protein content, it is grown in Southern and Eastern Asia, Central Africa and in some regions of South and North America, China and Australia. It is also known as chop suey bean, green gram, and golden gramme. Mungbean is mainly cultivated for humans (as dried beans or fresh sprouts), but it can also be used as a crop for green manure

and as cattle feed. Mungbean is a warm-season annual legume that is typically produced in rotation alongside grains like wheat and rice. Pods have 8 to 15 seed grains in them. The mungbean is sown in the latter week of June to the middle or first week of July. Mungbean should be planted for the summer or spring crop after the previous crop has been harvested (such as potatoes, sugarcane, mustard, cotton, etc.).

Okra [*Abelmoschus esculentus* (L.) Moench], also known as Lady Finger, is an annual plant in the Malvaceae family which is originally added in genus *hibiscus*. This genus is significant due to the existence of two cultivated species, *A. esculentus* and *A. caillei* (Patil *et al.*, 2015). More than 99% of the okra cultivation occurs exclusively in developing Asian and African countries, with a very low productivity. The states in India where it is widely grown are West Bengal, U. P., Bihar and Orissa. Okra, which is known as the key component of a well-balanced diet because of fibres and amino-acid content, has high tryptophan and lysine. The okra seeds have also acquired popularity as a novel source of oil and protein (Gemede *et al.*, 2015). It also includes significant levels of magnesium, iron, manganese and calcium, as well as vitamins.

## MATERIALS AND METHODS

Chemicals including ferric chloride hexahydrate ( $\text{FeCl}_3 \cdot 6\text{H}_2\text{O}$ ), ethanol ( $\text{C}_2\text{H}_5\text{OH}$ ), sodium borohydride ( $\text{NaBH}_4$ ), nitric acid ( $\text{HNO}_3$ ), perchloric acid ( $\text{HClO}_4$ ), sodium hypochlorite ( $\text{NaClO}$ ) and distilled water were used. Seeds of mungbean (Variety MH-421) were purchased from Krishi Vigyan Kendra, Rohtak (Haryana) and Okra (variety Arka Anamika) from local market in Rohtak (Haryana).

Iron oxide nanoparticles were synthesized by using chemical reduction method (Chaki *et al.*, 2015). 0.5406 g of ferric chloride hexahydrate ( $\text{FeCl}_3 \cdot 6\text{H}_2\text{O}$ ) was taken and dissolved in 4:1 ratio ethanol/water solution by well stirring. Sodium borohydride ( $\text{NaBH}_4$ ) solution was prepared by dissolving 0.3783 g of  $\text{NaBH}_4$  in 100 ml of deionized water. Black solid particles appeared immediately after the addition of first drop of sodium borohydride solution, and the remaining sodium borohydride was completely added to accelerate the reduction reaction. After adding the entire borohydride solution,

the mixture was stirred for another 10 min. The mixture was allowed to sit overnight and further separated through filtration using distilled water and ethanol. Finally, the nanoparticles were dried overnight in hot air oven at 323 K and were later used for characterization.

Characterization of synthesized iron oxide nanoparticles was done using various techniques. Absorbance peak of synthesized iron oxide nanoparticles was measured using UV-1800, UV spectrophotometer, Shimadzu to confirm the nano scale formation which showed absorption peak at 268 nm. Zeta analyzer was measured using Malvern Zetasizer Nano ZS which revealed the size and charge stability of the particle and the colloidal stability were predicted based on zeta potential magnitude. The structural properties of synthesized nanoparticles were characterized by using Scanning electron microscope (SEM; JSM-6390 LV, JEOL). The elemental composition was identified by energy dispersive X-ray spectroscopy system (EDS) using X-act (Oxford Instruments) coupled to the SEM. Fourier- transform infrared spectroscopy (FTIR) analysis was done using FTIR Spectrometer (Shimadzu) for testing some specific functional groups.

For the germination test, mungbean and okra seeds were surface-sterilized for 10 min with a 0.5% NaClO solution, washed five times with deionized water, and then dried with filter paper. Then filter paper was placed in each petri dish and each petri dish (diameter 90 mm) was filled with five ml of suspension, and ten selected seeds were evenly distributed in three replicates. The seeds were grown in an artificial climate incubator in the dark at 25°C and 70% relative humidity. The loss of water evaporated was supplied every 24 h (Libralato *et al.*, 2016; Sun *et al.*, 2019).

Radicles were considered to have germinated when they exceed half of the length of the seed (Sun *et al.*, 2019). For five days, the germinated seeds number was counted every 24 h. Seed germination percentage was calculated by using equation where number of seeds germinated was divided by total number of seeds taken and multiplied by 100.

$$\text{Seed germination rate (\%)} = \frac{\text{Number of seed germinated}}{\text{Total number of seeds taken}} \times 100$$

The following equation was used to calculate the germination index by comparing the sample's seed germination and root elongation to the control (Luo *et al.*, 2018).

$$\text{Germination index} = \frac{G_s \times L_s}{G_c \times L_c}$$

Where;  $G_c$  = Seed germination rate of control (%),  $L_c$  = Root length of control (cm),  $G_s$  = Seed germination rate and  $L_s$  = Root length (cm).

After growth of five days, seedling shoot and root elongations were measured after harvesting the shoots and roots separately. Fresh shoots and roots were washed and their weight was recorded. Dry biomass was recorded after oven drying the shoot and root samples. The dried plant samples were digested with 10 ml of digestion reagent (Nitric acid : Perchloric acid in 3 : 1). Acid digestion was performed on a hot plate at 70-100°C until yellow nitric chloride fumes and white perchloric acid fumes were produced. The digestion process was repeated until a clear solution remained after acid volatilization. When the residue in the flask became transparent, the digestion was stopped. Distilled water was used to dissolve the digested samples, which were then filtered to remove impurities. Using distilled water, a volume of 50 ml of solution was created. The samples were analyzed using an Atomic Absorption Spectrophotometer to determine the level of iron content in root shoot seedlings of okra and mung bean germinated seeds (Sun *et al.*, 2019). For measurement of translocation of iron in mungbean and okra translocation factor was calculated by using iron concentrations of shoot and root parts.

Translocation factor = Fe conc. in plants shoots / Fe conc. in plants roots

## RESULTS AND DISCUSSION

The zeta potential is described as the electric potential at the surface of shear proportion to that in the faraway bulk medium, is frequently used to describe the surface charge of iron nanoparticles. Surface charge is the major factor that determines the movement of particles in an electrical field. The particle size distribution by intensity shows iron oxide nanoparticle formation peak at 50.75 nm as

shown in Fig. 1 and zeta potential was found to be negative 24.1 mV. In general zeta potential higher than positive 30 mV and lower than negative 30 mV had high stability. Zeta potential values are prone to agglomeration due to interparticle interactions in dispersion with less than positive 25mV and greater than negative 25mV (Kumar and Dixit, 2017) and may result in physical instability (Mehta *et al.*, 2014). The result of zeta analyzer concluded that synthesized iron oxide nanoparticles were agglomerated.

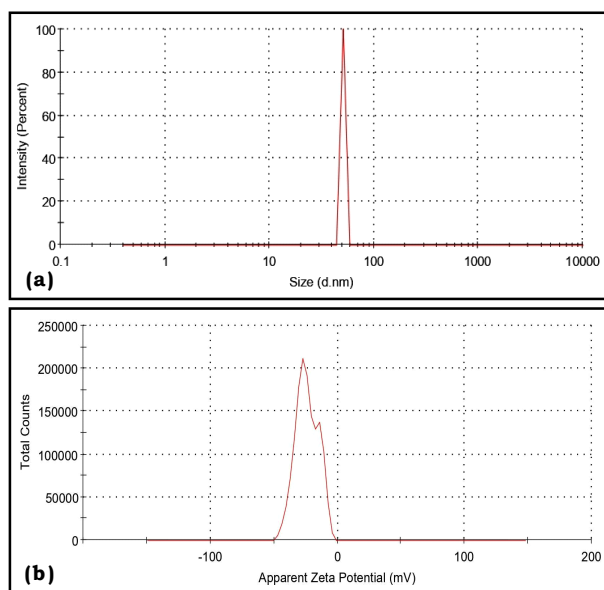


Fig. 1. (a). Particle size distribution and (b) Zeta size distribution of iron oxide nanoparticles.

Scanning Electron Microscopy (SEM) was used to reveal information about atom composition as well as topographic details of samples. As the biological behaviour of the NPs was highly dependent on size and shape, SEM played a crucial role in exploring the NPs' structural morphology. Fig. 2 (a) and (b) shows that the synthesized iron nanoparticles were made up of spherical shape at 1 and 5  $\mu$ m, respectively. The iron oxide nanoparticles were in form of nanospheres which were agglomerated.

The EDS of iron nanoparticles was done for determining the chemical composition. Its analysis creates data as a spectra, with peaks corresponding to the components of the analyzed sample. Its spectrum shows intense peaks of iron between 6.0-8.0 KeV, oxygen between range of 1.0-2.0 KeV, carbon and chlorine as well. Atomic percentage as represented by EDS spectrum was Fe (40.21%),

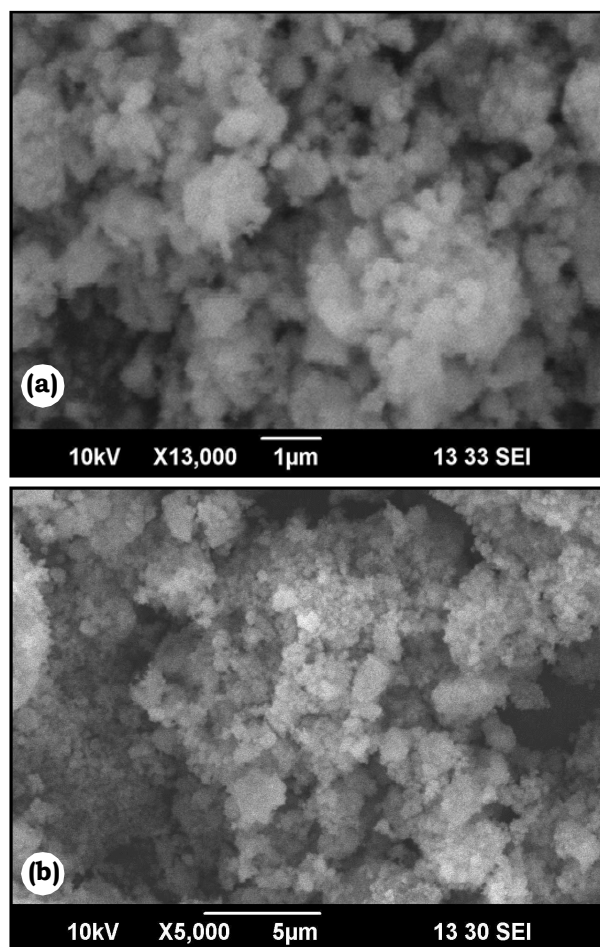


Fig. 2. SEM images of iron oxide nanoparticles at (a) 1  $\mu$ m and (b) 5  $\mu$ m, respectively.

O (51.08%), Na (6.21%) and Cl (2.50%) as shown in Fig. 3. Oxygen was also present suggesting surface oxidation of the FeNPs. Similar results were reported by Saqib *et al.* (2019).

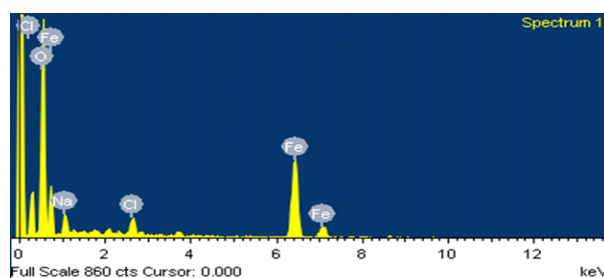


Fig. 3. EDS spectrum of synthesized iron oxide nanoparticles.

Fourier Transform Infrared Spectroscopy (FTIR) analysis was done to analyze the presence of functional groups of synthesized iron oxide nanoparticles. The infrared spectrum obtained was in range of 500-4000/ $\text{cm}^{-1}$  as shown in Fig. 4 which identified chemical bonds as well as the functional



Fig. 4. Representation of FTIR of synthesized iron oxide nanoparticles.

groups present in the compound. The FTIR report of FeNPs showing broad peak at 3414.47/cm referred to O-H stretch of H bonding in alcohol and phenols. The absorption peaks at 1708/cm and 1453.81/cm were due to symmetric and asymmetric bending vibration of C=O and peak at 1107.72/cm represented C-O stretching vibration of primary alcohols (Farahmandjou and Soflaee, 2015).

The mungbean seeds started growing on first day and till final day showing 100% germination rate in control, 450 and 600 mg/l. In okra, no germination was observed on first day but the seeds started to grow from second day and maximum germination rate was observed at 450 mg/l iron oxide nanoparticles treated concentration. The germination index was observed maximum in okra and mungbean

seeds at 450 and 600 mg/l iron oxide nanoparticle concentrations respectively as shown in Fig. 5 (a) and (b). No inhibition of growth was observed in treated seeds with iron oxide nanoparticles (Sun *et al.*, 2019).

In mungbean seeds germination study, maximum root-shoot length was observed at 150 and 600 mg/l concentration and caused no significant negative effects. In okra seeds, maximum growth of root-shoot length was observed at 450 mg/l concentration (Fig. 6 a and b). The shoot root length was found to be similar as per the previous research which showed maximum growth at higher concentration (Dwivedi *et al.*, 2018; Sun *et al.*, 2020).

After germination fresh weight and dry weight was observed for both the seeds, in mung bean seeds (maximum fresh weight was observed at 150 mg/l concentration and minimum fresh weight was observed at 600 mg/l concentration). In okra seeds, maximum fresh weight was observed at 450 mg/l concentration and minimum fresh weight was observed at 600 mg/l concentration. In mungbean, seeds maximum dry weight was observed at 150 mg/l concentration and minimum dry weight was observed at 600 mg/l concentration. In okra seeds, maximum dry weight was observed at 450 mg/l concentration and minimum dry weight was observed at 600 mg/l iron oxide nanoparticles concentration (Fig. 7 a and b). Similar results were shown in previous findings (Iannone *et al.*, 2016; Libralato *et al.*, 2016; Dwivedi *et al.*, 2018; Sun *et al.*, 2019,

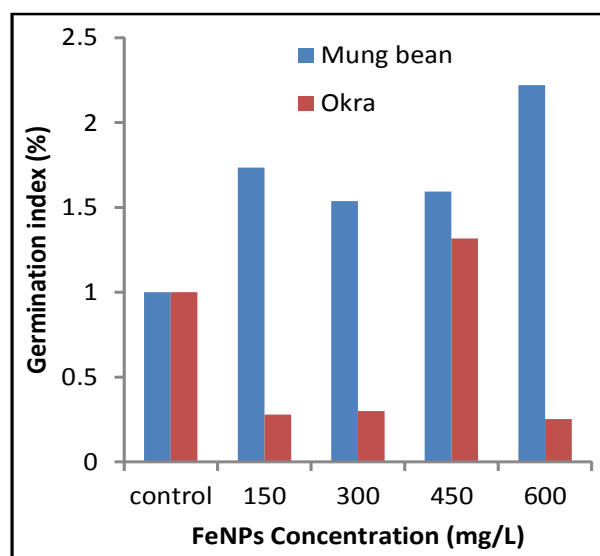
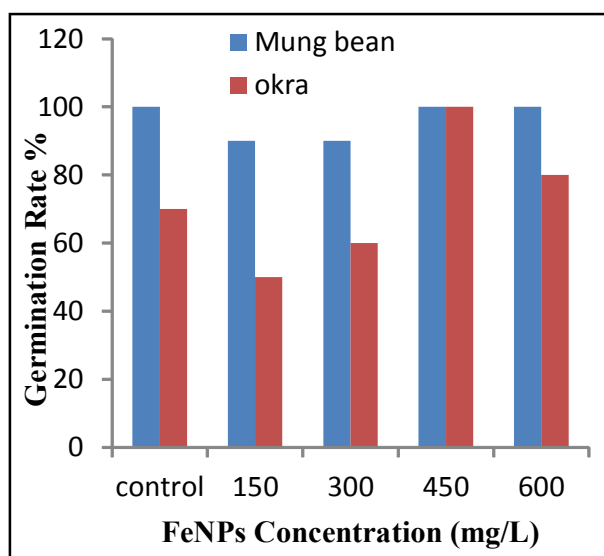


Fig. 5 (a). Germination percentage and (b) germination index in mungbean and okra seeds after 5 days.

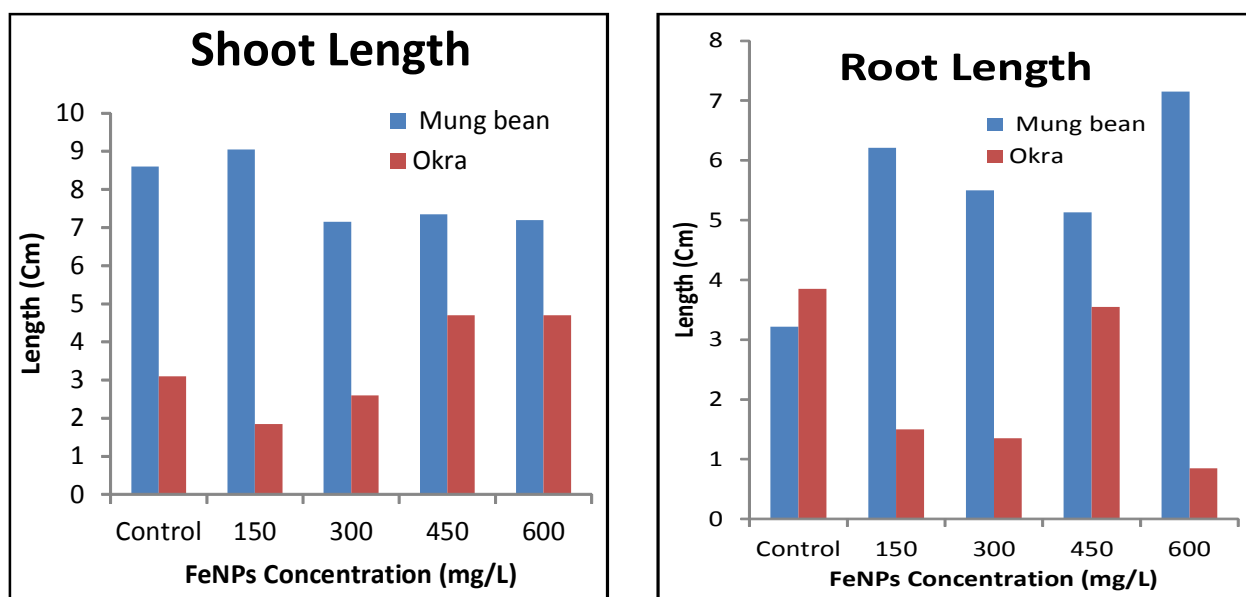


Fig. 6. Comparison of (a) shoot and (b) root length of mungbean and okra seeds after germination.

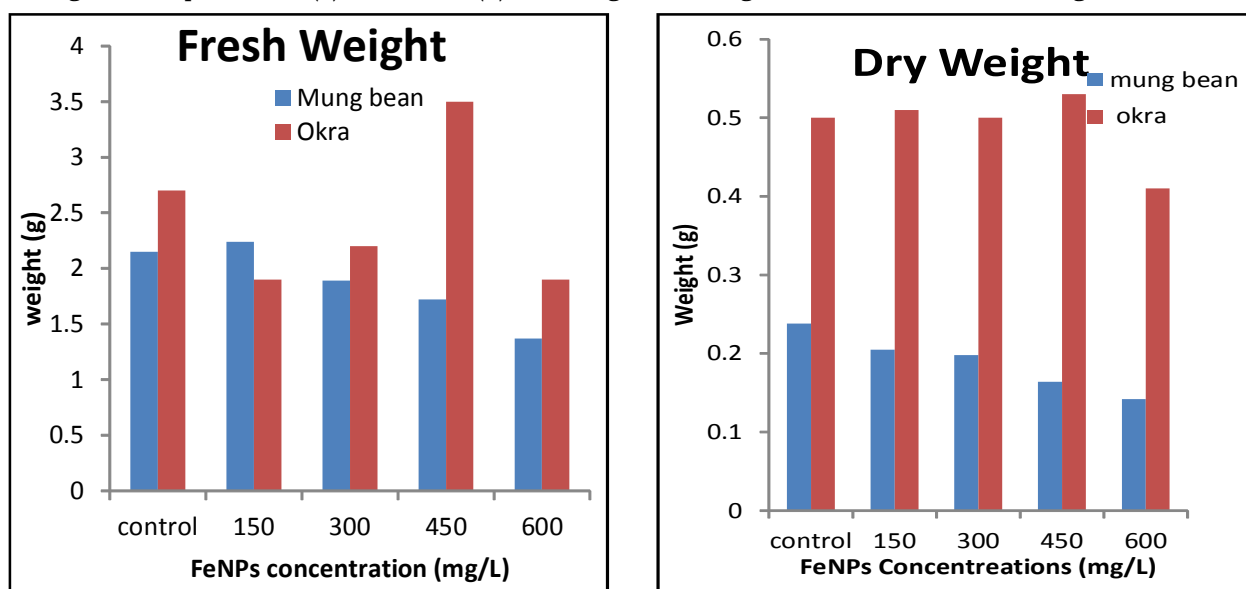


Fig. 7 (a). Fresh and (b) dry weight in mungbean and okra seed after germination.

2020). Further, it was observed that higher concentration i.e. 600 mg/l of iron oxide nanoparticles inhibited the biomass of germinated seeds.

The dried parts of roots and shoots roots and shoots were acid digested and iron concentration was recorded by using Atomic Absorption Spectrophotometer. The iron concentration present in shoots and roots of mung bean and root part of okra generally showed higher concentration of iron (Fig. 8a and b). The higher iron content of shoot in mung bean was observed at 600mg/L while in okra, it was observed at 300mg/L. Compared

to the control maximum concentration of iron in root part was measured at 600 mg/l iron oxide nanoparticles treated mungbean and okra. Translocation factor is a shoot-root quotient which explains the ability of a plant to translocate metal forms from roots to shoots and shoots to leaves. The translocation factor in okra and mungbean was highest at 300 and 450 mg/l iron oxide nanoparticles concentrations, respectively (Fig. 9).

It was found that all the iron oxide iron oxide nanoparticles treated seeds both in mungbean and okra had higher concentration of iron especially in root part and translocation factor

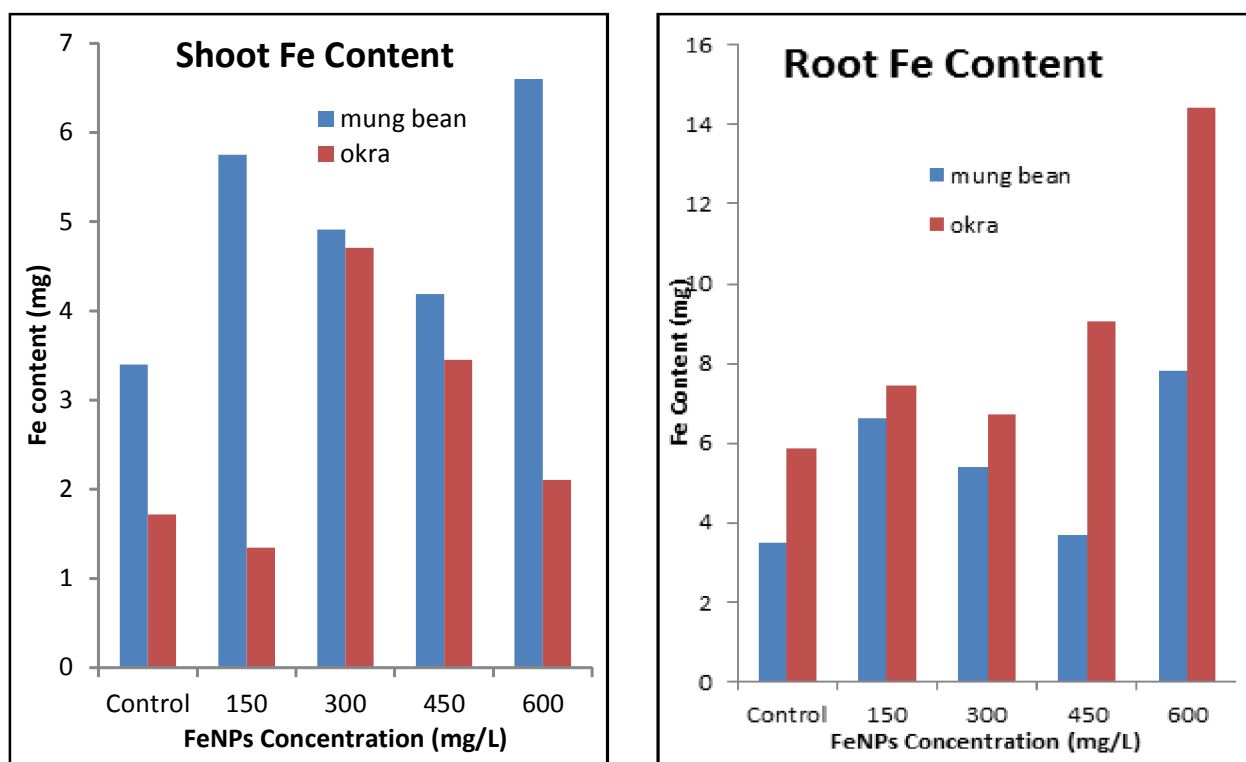


Fig. 8. Iron content in (a) shoot and (b) root of mung bean and okra.

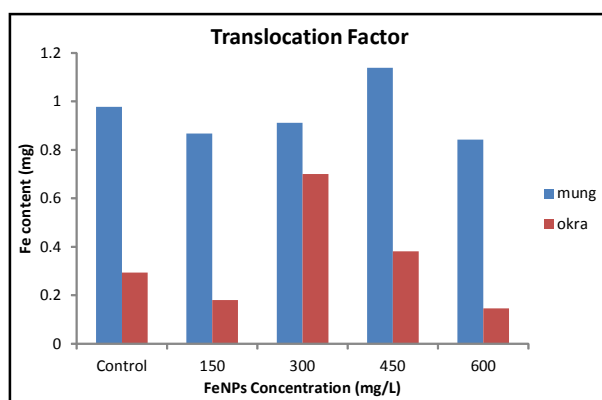


Fig. 9. Translocation factor in mungbean and okra seeds.

was much lower in all treated seeds accumulated in root part and due to their high surface area, small particle size and sorbing capacity attached to root surface. It was found in previous research that plants exposed to  $n\text{Fe}_3\text{O}_4$  had elevated Fe concentrations in their roots but not in their shoots, indicating that the nanoparticles were unable to be translocated to the shoots. Additionally, iron oxide nanoparticles accumulation in the roots was observed, but Fe is a not transferrable form and has a low mobility, so it was not transported to the shoots (Sun *et al.*, 2019).

## CONCLUSION

Iron nanoparticles were synthesized by chemical reduction method to study their effect on seed germination of mungbean and okra seeds. Synthesized iron oxide nanoparticles morphology was determined by using different characterization techniques such as UV-Vis spectroscopy, Zeta potential, Scanning electron microscopy (SEM), and Electron dispersive spectroscopy (EDS). UV-Vis analysis confirmed the reduction of metallic (Ferric chloride) solution into iron oxide nanoparticles. UV-Vis showed peak at 280 nm which confirmed the formation of iron nanoparticles. Zeta analyzer showed particle size distribution peak at 50.97 nm and negative 24.1 mV zeta potential which confirmed the stability of iron nanoparticles. SEM showed formation of iron nanoparticles in spherical shape at 1 and 5  $\mu\text{m}$ . EDS spectrum showed intense peaks of iron between 6 to 8 KeV. FTIR report of FeNPs showing broad peak at 3414.47/cm referring to O-H stretch of H bonding in alcohol and phenols, peak at 1453.81/cm was due to de-ionized water used as solvent and peak at 1107.72/cm representing C-O stretching vibration of primary alcohols. The seeds showed positive



results in germination parameters i.e. root shoot elongation, total biomass but the iron content and translocation factor showed excess iron accumulation in okra and mungbean at 300 and 450 mg/l concentration when treated with iron oxide nanoparticle solution. However, iron in roots was poorly translocated to the shoot part. In agriculture, nanoparticles are used as fertilizers and nanopesticides to protect products and nutrients level to increase the yield without decontamination of soil, water and guard against numerous insects and microbial diseases and pest. Consequently, this method contributed to a decrease in environmental pollutants.

## ACKNOWLEDGEMENT

The authors are thankful to Dean Students' Welfare, Maharshi Dayanand University for providing a minor research project under Dr. Radha Krishanan Foundation Fund.

## REFERENCES

- Briat, J. F., Dubos, C. and Gaymard, F. (2015). Iron nutrition, biomass production and plant product quality. *Trends Plant Sci.* **20**: 33-40.
- Chaki, S. H., Malek, T. J., Chaudhary, M. D., Tailor, J. P. and Deshpande, M. P. (2015). Magnetite Fe<sub>3</sub>O<sub>4</sub> nanoparticles synthesis by wet chemical reduction and their characterization. *Adv. Nat. Sci. Nanosci.* **6**: 035009. DOI: 10.1088/2043-6262/6/3/035009.
- Da Costa, M. V. J. and Sharma, P. K. (2016). Effect of copper oxide nanoparticles on growth, morphology, photosynthesis and antioxidant response in *Oryza sativa*. *Photosynthetica* **54**: 110-119.
- Dwivedi, A. D., Yoon, H., Singh, J. P., Chae, K. H., Rho, S. C., Hwang, D. S. and Chang, Y. S. (2018). Uptake, distribution and transformation of zerovalent iron nanoparticles in the edible plant *Cucumis sativus*. *J. Environ. Sci. Technol.* **52**: 10057-10066.
- Farahmandjou, M. and Soflaee, F. (2015). Synthesis and characterization of  $\alpha$ -Fe<sub>2</sub>O<sub>3</sub> nanoparticles by simple co-precipitation method. *Phys. Chem. Res.* **3**: 191-196.
- Gemedé, H. F., Ratta, N., Haki, G. D., Woldegiorgis, A. Z. and Beyene, F. (2015). Nutritional quality and health benefits of okra (*Abelmoschus esculentus*): A review. *J Food Process Technol.* **14**: 2.
- Iannone, M. F., Groppa, M. D., de Sousa, M. E., van Raap, M. B. F. and Benavides, M. P. (2016). Impact of magnetite iron oxide nanoparticles on wheat (*Triticum aestivum* L.) development: Evaluation of oxidative damage. *Environ. Exp. Bot.* **131**: 77-88.
- Khan, I., Saeed, K. and Khan, I. (2019). Nanoparticles: Properties, applications and toxicities. *Arab. J. Chem.* **12**: 908-931.
- Kumar, A. and Dixit, C. K. (2017). Methods for characterization of nanoparticles. In: *Advances in Nanomedicine for the Delivery of Therapeutic Nucleic Acids*. pp. 43-58. Woodhead Publishing.
- Lei, C., Sun, Y., Tsang, D. C. and Lin, D. (2018). Environmental transformations and ecological effects of iron-based nanoparticles. *Environ. Pollut.* **232**: 10-30.
- Libralato, G., Devoti, A. C., Zanella, M., Sabbioni, E., Micetic, I., Manodori, L. and Ghirardini, A. V. (2016). Phytotoxicity of ionic, micro- and nano-sized iron in three plant species. *Ecotoxicol. Environ. Saf.* **123**: 81-88.
- Luo, Y., Liang, J., Zeng, G., Chen, M., Mo, D., Li, G. and Zhang, D. (2018). Seed germination test for toxicity evaluation of compost: Its roles, problems and prospects. *J. Waste Manag.* **71**: 109-114.
- Mehta, M., Shah, J., Khakhkhkar, T., Shah, R. and Hemavathi, K. G. (2014). Anticonvulsant hypersensitivity syndrome associated with carbamazepine administration: Case series. *J. Pharmacol. Pharmacother.* **5**: 59-62.
- Patil, P., Sutar, S., Joseph, J. K., Malik, S., Rao, S., Yadav, S. and Bhat, K. V. (2015). A systematic review of the genus *Abelmoschus* (Malvaceae). *Rheedeia* **25**: 14-30.
- Rout, G. R. and Sahoo, S. (2015). Role of iron in plant growth and metabolism. *Agric. Rev.* **3**: 01-24.
- Saqib, S., Munis, M. F. H., Zaman, W., Ullah, F., Shah, S. N., Ayaz, A. and Bahadur, S. (2019). Synthesis, characterization and use of iron oxide nano particles for antibacterial activity. *Microsc. Res. Tech.* **82**: 415-420.
- Sarmast, M. K. and Salehi, H. (2016). Silver nanoparticles: An influential element in plant nanobiotechnology. *Mol. Biotechnol.* **58**: 441-449.
- Siddiqui, M. H., Al-Whaibi, M. H., Firoz, M. and Al-Khaishany, M. Y. (2015). Role of nanoparticles in plants. *Nanotechnology and Plant Sciences*. pp. 19-35.



- Sun, Y., Jing, R., Zheng, F., Zhang, S., Jiao, W. and Wang, F. (2019). Evaluating phytotoxicity of bare and starch-stabilized zero-valent iron nanoparticles in mungbean. *Chemosphere* **236**: 124336.
- Sun, Y., Wang, W., Zheng, F., Zhang, S., Wang, F. and Liu, S. (2020). Phytotoxicity of iron-based materials in mung bean: Seed germination tests. *Chemosphere* **251**: 126432.
- Tighe-Neira, R., Carmora, E., Recio, G., Nunes-Nesi, A., Reyes-Diaz, M., Alberdi, M. and Inostroza-Blancheteau, C. (2018). Metallic nanoparticles influence the structure and function of the photosynthetic apparatus in plants. *Plant Physiol. Biochem.* **130**: 408-417.
- Tighe-Neira, R., Gonzalez-Villagra, J., Nunes-Nesi, A. and Inostroza-Blancheteau, C. (2022). Impact of nanoparticles and their ionic counterparts derived from heavy metals on the physiology of food crops. *Plant Physiol. Biochem.* **172**: 14-23.
- Tripathi, D. K., Singh, S., Singh, S., Pandey, R., Singh, V. P., Sharma, N. C. and Chauhan, D. K. (2017). An overview on manufactured nanoparticles in plants: Uptake, translocation, accumulation and phytotoxicity. *Plant Physiol. Biochem.* **110**: 02-12.
- Yirsaw, B. D., Megharaj, M., Chen, Z. and Naidu, R. (2016). Environmental application and ecological significance of nano-zero valent iron. *J. Environ. Sci.* **44**: 88-98.
- Zahra, N., Hafeez, M. B., Shaukat, K., Wahid, A. and Hasanuzzaman, M. (2021). Fe toxicity in plants: Impacts and remediation. *Physiol. Plant.* **173**: 201-222.
- Zargar, S. M., Agrawal, G. K., Rakwal, R. and Fukao, Y. (2015). Quantitative proteomics reveals role of sugar in decreasing photosynthetic activity due to Fe deficiency. *Front. Plant Sci.* **6**: 592.